

# Chapter 1

## Experimental Nanophotothermolysis of Human Pancreatic Cancer Cells Using Gold Nanoparticles



Lucian Mocan<sup>1</sup>, Lucia Agoston-Coldea<sup>2</sup>, Teodora Mocan<sup>3</sup>,  
Cristian T. Matea<sup>3</sup>, Flaviu A. Tabaran<sup>4</sup>, Teodora Pop<sup>1</sup>,  
Ofelia Mosteanu<sup>1</sup>, Cornel Iancu<sup>1</sup>

<sup>1</sup>Gastroenterology Institute; "Iuliu Hatieganu" University of Medicine and Pharmacy, 19-21 Croitorilor Street, Cluj-Napoca, Romania, 400162

<sup>2</sup>Department of Medical Sciences, Iuliu Hatieganu University of Medicine & Pharmacy, 2-4 Clinicilor, 400006, Cluj-Napoca, Romania

<sup>3</sup>Department of Physiology, "Iuliu Hatieganu" University of Medicine and Pharmacy, Clinicilor 5-7, Cluj-Napoca, Romania

<sup>4</sup>Department of Pathology, University of Agricultural Sciences and Veterinary Medicine, Faculty of Veterinary Medicine, 3-5 Manastur Street, 400372 Cluj-Napoca, Romania

---

## Introduction

Pancreatic cancer (PC) represents the fourth leading cause of cancer death worldwide, having an overall 5-year survival rate of less than 5%. (1) At the current time, the surgical resection of the primary tumor is the only therapeutically approach that provides improvement in survival. Moreover, PC is also one of the most intrinsically drug-resistant of all tumors and the lack of effective cytostatics contributes to the increased mortality rates. (2)

An exciting and new approach to PC treatment is represented by the targeted therapeutics systems (an active molecule attached to a molecular carrier). The use of these biological carriers for the development of specific and sensitive site-targeted bio-nanosystems makes the selective internalization of molecules with photothermal properties in cancer cells possible. This internalization process is not possible under normal conditions (3) (4) Generally, the use of targeting molecules such as antibodies, folates and growth factors, has been specifically proposed for carrying nanomaterials to the cancer cells and tumors.

However, 100% selective internalization of nanobioconjugates in the cancer cells remains problematic.

Nanomediated photothermal therapy is a minimally-invasive treatment method in which photon energy from activated nanoparticles is converted to heat in tumor-loaded tissues (elevated to 40–43 °C and above). By using this method, highly efficient intratumoral heating can be achieved by non-radiative relaxation through electron–phonon and subsequent phonon–phonon coupling processes. The use of such particles in near-infrared PTT is highly attractive due to their rapid synthesis, facile bioconjugation, strong absorption cross-section, and tunable optical extinction. (5)

Recently, gold nanoparticles were approved on human treatment in phase 1 clinical trials, which suggests that gold can act as an effective and safe therapeutic agent. ([www.clinicaltrials.gov](http://www.clinicaltrials.gov)). Furthermore, light absorbing properties of gold nanoparticles has been used to produce localized lysis to malign cells at sublethal levels by changes in cellular functions. (6)

## **In Vitro Treatment of Pancreatic Cancer Using Human Serum Albumin-Coated Gold Nanoparticles (HSA-GNPs)**

We previously developed and published a novel system of PT for PC mediated by multiwalled carbon nanotubes (MWCNTs) bound to human serum albumin (HSA). (7, 8) This recent idea operates under the hypothesis that HSA molecules increase the effectiveness of carbon nanotubes internalization inside malign cells. Still, our published studies suggest that carbon nanotubes bound to human serum albumin exhibit a certain toxicity and are not 100% selective for malign cells. Moreover our current research in targeting pancreatic cancer with

human serum albumin (HSA) bound to gold nanoparticles accepted for administration in humans that epithelial non- malign cells exhibit high uptake rates of GNP-HSA.

In this context, considering the described role of gold nanoparticles in human diagnosis and treatment applications, we reasoned that the development of novel selective targeted bio- nanosystems based on gold nanoparticles bound to novel specific antibodies, will allow us the discovery of a feasible treatment that may be successfully introduced in clinical trials on patients with PC. (9)

## **Synthesis of Gold Nanoparticles**

Gold nanoparticles were synthesized according to standard wet chemical methods, using sodium borohydride as reducing agent. Briefly, the adding of 50 ml of aqueous solution containing 4.3 mg solid sodium borohydride to 100 ml of aqueous solution containing 100  $\mu\text{mol/L}$  hydrogen tetrachloroaurate was done in a typical experiment, under vigorous stirring, continued overnight. Gold nanoparticles thus formed were filtered through a 0.22  $\mu\text{m}$  filter and used for experiments.

## **Human Serum Albumin-Modified Gold Nanoparticles**

In a few words, human serum albumin (HSA) - gold nanoparticle (GNPs) conjugates were obtained using poly-ortho-pyridyl disulfide, 2.000 Da (ethylene glycol)-N-hydroxysuccinimide as linker. Polyethylene glycol (PEG)-antibody conjugates were prepared by reacting one part 125  $\mu\text{M}$  OPSS PEG-NHS with 9 parts 1 mg/ml antibody at 4  $^{\circ}\text{C}$  overnight. Gold nanoparticles were suspended in Milli-Q water and exposed to PEG-antibody conjugates for 1 hour, at 4  $^{\circ}\text{C}$ , at a volume ratio of 100:1. Following antibody coupling, GNPs

were reacted using a solution of mPEG-SH (5 mM, 5,000 Da), for at least 4 hours, at a temperature of 4 °C (1:200 volumetric ratio) to stabilize any exposed gold surface area. After PEG and/or antibody modification, GNPs were centrifuged to remove free molecules, aspirated and suspended in phosphate buffered saline (PBS) to an optical density of 2.0 ( $4.2 \times 10^{11}$  particles/ml).

Universal attenuated total reflectance fourier transform infrared spectroscopy (ATR-FT-IR) was performed using a Perkin-Elmer Spectrum Two® instrument with an UATR single reflection diamond. Baseline corrections and spectra processing were done using the instruments Spectrum 10™ software.

Atomic force microscopy measurements were carried out on a Workshop TT-AFM® (AFMWorkshop, CA, USA) in vibrating mode using ACTA-SS cantilevers (AppNano, CA, USA). Samples were deposited on a mica substrate using a KLM® SCC spin coater. The recorded data was processed with the aid of Gwyddion® 2.36 software.

The obtained HSA stabilized gold nanoparticles were subjected to UV-Vis and DLS measurements.

AFM measurements were conducted on the GNP-HSA sample in order to further investigate the size and shape of the obtained nanoparticles. Figure 1 A. shows a 2D representation of GNP-HSA, spherical nanoparticles can be observed with an average diameter of ~41nm.

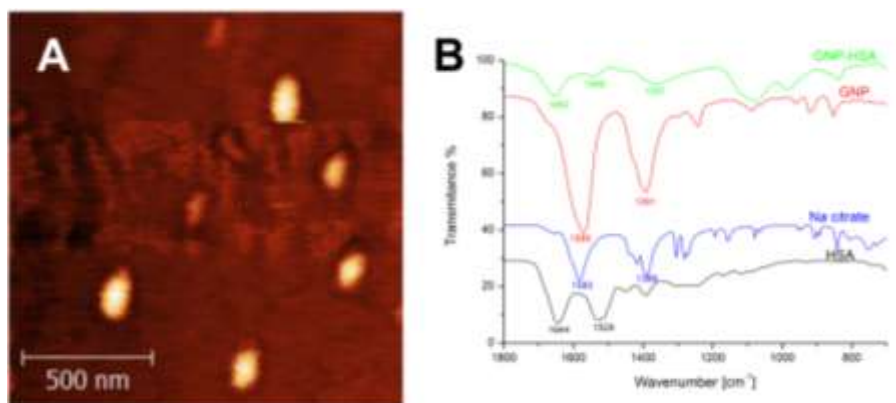


**Figure 1.** AFM measurements of GNP-HSA: A. 2D image of HSA functionalized GNPs; B. FT- IR spectra of HSA functionalized gold nanoparticles (GNP-HSA), citrate stabilized GNP, Na citrate and HSA protein.

In order to confirm the successful attachment of HSA on the gold nanoparticle surface, ATR-FT- IR spectroscopy measurements were undertaken. Figure 1B depicts FT-IR spectra of GNP-HSA, GNP, sodium citrate and HSA. For the GNP-HSA sample the two characteristic bands of HSA can be observed at  $1652\text{ cm}^{-1}$  and  $1546\text{ cm}^{-1}$  attributed to the amide I and amide II, respectively. The band at  $1652\text{ cm}^{-1}$  is attributed to C=O stretching from the albumin, while the band at  $1546\text{ cm}^{-1}$  is a coupling of C-N stretching and N-H bending modes in the protein. In the case of citrate capped GNPs the bands corresponding to the symmetric and antisymmetric stretching of  $\text{COO}^-$  of the citrate ions, can be observed at  $1391\text{ cm}^{-1}$  and  $1569\text{ cm}^{-1}$ , respectively. Figure 1 indicates that the citrate ions from the GNPs surface were replaced by HSA during the functionalization step of the gold nanoparticles. This phenomena can be explained by the fact that HSA has a tertiary structure stabilized by 17 internal disulphide bonds between 34 cysteine residues which accounts for the higher affinity of the protein for gold nanoparticles, compared to that of citrate ions.

## Development of the *in Vitro* Test Platform

The human pancreatic adenocarcinoma 1.4E7 cell line was used for the experiments. This is a stable hybrid cell line formed by the electrofusion of human pancreatic islets with the human pancreatic ductal carcinoma cell line (PANC-1 cells), purchased from the European Collection of Cell Cultures (ECACC). Cells were grown in 25 cm<sup>3</sup> plastic flasks and maintained (in a humidified 37 °C 5% CO<sub>2</sub> incubator) in RPMI containing 10% fetal bovine serum with 1% penicillin-streptomycin. Cells were kept in logarithmic growth phase by routine passage every 2-3 days. On reaching confluence, cells were separated after being washed with phosphate buffered saline and they were detached using trypsin. For the experiments, cells were grown to confluence on glass Lab-Tek 4 chamber slides (No.177399). Albumin-coated gold nanoparticles were further delivered to adherent cell cultures, after removal of the cell culture medium, and incubated for gradually increased periods of time (1 minute, 30 minutes, 1 hour, 5 hours, 24 hours) at increasing concentrations: 1 mg/L, 5 mg/L, 20 mg/L, 50 mg/l. For each concentration, all experiments were carried out in triplicate. Figure 2 shows the intracellular "uptake" of gold nanoparticles (appearing on phase contrast microscopy as black intracytoplasmic conglomerations) functionalized with human serum albumin into malignant pancreatic cells. As suggested by the images below, we have observed (by both phase contrast microscopy and fluorescence microscopy) an intracellular internalization directly proportional to the concentration of nanoparticles in the solution administered. In addition, the quantification of intracellular gold nanoparticles conglomerations using fluorescence (by marking the nanobioconjugate with fluorescent molecules of fluorescein isothiocyanate) shows the selectivity of the uptake process compared to the simple FITC-labeled GNP solution.

For immunohistochemistry, Lab-Tek chamber slides were used for in situ



observation of glass- adherent cells (walls were removed and the AuNP medium/solution cleared). Thus, no cell transfer was necessary before visualization/staining. After administration and irradiation, cells were washed 3 times with 1 x PBS and then fixed with 10% formaldehyde solution for 10 minutes, washed three times with PBS and subjected to chemical immunostaining. Cultured cells were examined with an inverted phase contrast microscope (Olympus FSX100, Munich, Germany).

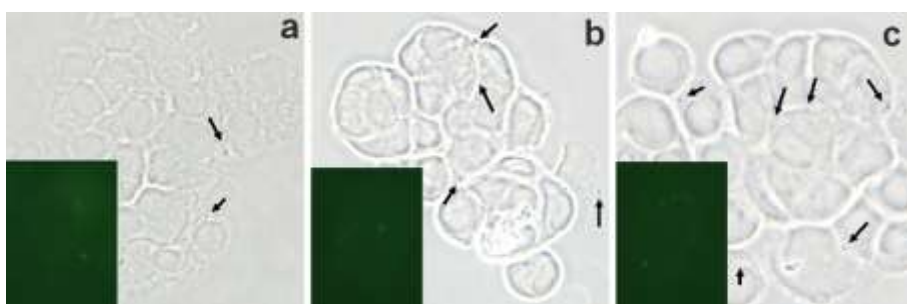


**Figure 2.**  $1.4E7$  pancreatic cancer cells incubated for 30 minutes with 1 mg/L-a, 5 mg/L of HSA-GNPs, visualized by phase contrast microscopy ( $\times 400$  magnification); bottom left: quantification using an inverted fluorescence microscope, green filter, 455 nm.

## Laser Treatment

A 2W laser (Apel Laser, Bucharest, Romania) operating at 808 nm was used for a 2-minute irradiation of a cell monolayer placed on a glass substrate (laboratory glass slides, after removal of secondary walls and discharge of HSA-coated AuNP solution), after having been incubated with nanomaterials for various time periods. The laser diode was positioned vertically, 2 cm away from the surface of the microtiter plate. For ex vivo preactivation of nanoparticles, the AuNP solution was placed in a Lab-Tek 177399 slide and similarly irradiated for different time periods (5, 10, 20 minutes). AuNP solution temperature was measured using a digital thermometer (Digitron 1804).

## Cell Proliferation

Following treatment, the MTT assay was performed to determine cell proliferation (3-[4,5-Dimethyl-2-thiazolyl]-2,5-diphenyl-2H-tetrazolium bromide). Briefly,  $1.4 \times 10^7$  cells were plated at a seeding density of  $4 \times 10^4$  cells/ml in 96-well plates. After being treated with different concentrations of nanoparticle solution (pre-irradiated or simple) at different time intervals, 10  $\mu$ l of MTT (5 mg/ml) were added to each well. Cultures were returned to the incubator and incubated for 4 hours at 37 °C. Further, the solution was removed and each well was added 100  $\mu$ l of MTT solvent. After stirring for 30 minutes, absorbance was measured at wavelengths of 570 nm by spectrophotometry, using a microplate reader (MW-520).

## Cytotoxicity Studies: Oxidative Stress Detection

The Total ROS/superoxide detection kit (Enzo Life Sciences, Plymouth Meeting, Pa, USA) was used to stimulate the production of reactive oxygen species (ROS) and/or reactive nitrogen species (RNS) in the cells exposed to GNPs, before and after treatment.  $1.47 \times 10^7$  adherent cells were incubated with GNPs for 30 minutes at 37 °C. Following incubation with GNPs (pre-activated/simple) +/- laser irradiation, cells were treated with reagent for oxidative stress detection for 30 minutes. Finally, cells were subjected to trypsinization and suspended with 0.5 ml of 10% FBS in  $1 \times$  wash buffer. Green fluorescence, an indicator of cellular production of different ROS/RNS types, was present in treated cells and visualized using the FACSCalibur flow cytometer (Becton Dickinson, San Jose, CA, USA) in the green FL1 channel (530 nm). All parameters considered for analysis were collected at low speed, in logarithmic mode (approx. 15 microliters  $\text{min}^{-1}$ ), in order to maintain the

counting level under 1,000 events per second. Characterization of cell population concentration was performed using both CellQuest software and PaintAGate. In addition, the accumulation of hydrogen peroxide was measured using CM-H<sub>2</sub>DCFDA (Invitrogen) and detected in the green channel (525 nm). Green fluorescent images were collected using the Olympus FSX100 fluorescence microscope. ROS species detection kit, Enzo Life Sciences, for flow cytometry, was used for the monitoring of real time release of reactive oxygen species and/or reactive nitrogen species (ROS/RNS) in 1.4E7 cells, before and after treatment. The kit contains the reagent for oxidative stress detection (green) as a marker detecting cell-penetrating ROS, which reacts with many reactive species, such as hydroxyl radical and hydrogen peroxide.

## **Analysis of the Mitochondrial Function**

1.4E7 cells were grown to confluence on Lab-Tek 4 chamber glass slides. A pre-heated (37 °C) dye solution containing MitoTracker® (Invitrogen) was added for 30 minutes, after removal of the culture medium (10). After staining was completed, cells were examined with an Olympus FSX100 microscope in the red channel. In order to further measure total mitochondrial mass, stained slides were scanned at a resolution of 100 µm by means of a proteomics imaging system (ProXPRESS 2-D, Perkin-Elmer, Boston, MA) with 480-nm excitation and 620-nm emission filters. The exposure time was adjusted to achieve a pixel intensity value of 55,000 to 63,000 on the more intense spots on the slides. Images were subsequently analyzed using Progenesis Discovery software, 2003 version. (Nonlinear Dynamics, Ltd., Newcastle upon Tyne, Great Britain). MitoTracker Red CMXRos is a red fluorescent dye (with a slightly thiol-reactive chloromethyl fraction), which stains mitochondria in living cells and thus, its passive intracellular diffusion depends on the

membrane potential function. Once the mitochondria are functionalized, cells can further be fixed with aldehyde-based fixative.

**Table 1.** Cytotoxic effects of different incubation times (%).

<b>Cytotoxicity of HSA-GNPs at various concentrations and various incubation times</b>				
	<b>1 min</b>	<b>1 hour</b>	<b>3 hours</b>	<b>24 hours</b>
HeLa Control	0%	0.4%	0.5%	1.7%
1.4E7 Control	0%	0.3%	0.7%	2.1%
HeLa 1 mg/L	0.3%	0.7%	1.6%	3.2%
1.4E7 1 mg/L	0.7%	1.1%	2.1%	3.4%
HeLa 5 mg/L	0.6%	1%	2.4%	4.5%
1.4E7 5 mg/L	0.5%	0.9%	2.3%	4.1%
HeLa 20 mg/L	0.8%	1.4%	3.2%	4.2%
1.4E7 20 mg/L	0.9%	1.4%	2.2%	4.1%
HeLa 50 mg/L	0.7%	1.3%	2.4%	4.5%
1.4E7 50 mg/L	1.4%	1.6%	2.2%	5.8%

## Assessing the Efficacy of Nanophotothermal Therapy

Cells grown in 6-well plates were treated with drugs for 48 h and incubated with 5 II Annexin V-Rhodamine in functionalization-compatible buffer (10 mM HEPES, 140 mM NaCl, 2.5 mM CaCl<sub>2</sub>, pH 7.4 ) for 15 minutes, in the dark, in accordance with the manufacturer's protocol. Cells were further washed in buffer, counterstained with propidium iodide and analyzed immediately using the Becton Dickinson FACSCalibur flow cytometer (488 nm and 585 nm excitation). Annexin V-Alexa Fluor 488, propidium iodide, or both, have been omitted for negative controls.

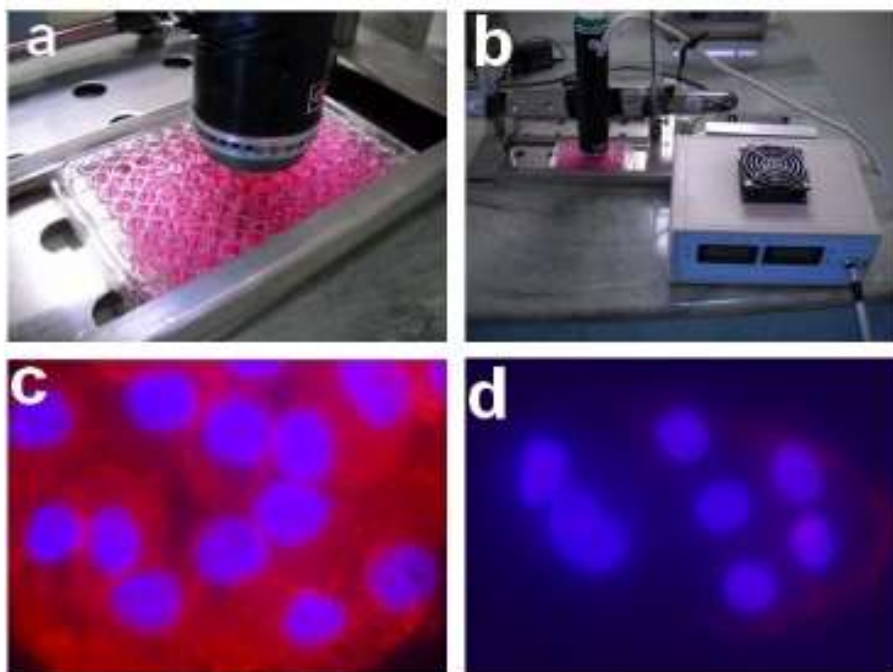


**Figure 3.** Nanophotothermal therapy of PANC-1 cells mediated by HSA-GNPs. a-b System settings c-d Annexin V expression in PANC-1 cells and CRL-4020 respectively (60 minutes exposure, 20 mg/L).

For the 30 minute assessment, cell necrosis increased from 58.34% (1 mg/L) to 90.34% (50 mg/L). In normal epithelial cells, the values obtained for the 30 minute samples were lower for all exposure concentrations. The significance of cytotoxicity threshold for CRL-4020 cells was set for a p value of <0.0001, for the 30 minute assessment, values ranging from 8.77% to 68.86% in all the concentration groups (1-50 mg/L).

Moreover, the values recorded for the 30 minute exposure period ranged from 6.08% to 62.23% for different concentrations for the PANC-1 group exposed to MWCNTs alone. The following levels of significance were calculated for the 30-minute exposure period and for 5 mg concentrations: PANC-1/CRL-4020:

70.78%/9.89% ( $p < 0.001$ ). As seen in Fig. 3, c-d, the optimal apoptotic effect after incubation with HSA-GNP was obtained for 5 mg/l. (PANC-1/CRL-4020: 56.1%/11.4% for the 60-second exposure period, and 75.34%/14.67% for the 30-minute exposure period. After 60 minutes of incubation, the difference in apoptosis was also big between the two cell lines at low/average GNP-HSA concentrations (80.12% - 1 mg/L, 86.14% - 5 mg/L, 85.82% - 20 mg/L for PANC-1, 15.56% - 1 mg/L, 21.34% - 5 mg/L, 52.14% - 20 mg/L for CRL-4020.) Cell lysis values for high nanomaterial concentrations were roughly similar (100% - PANC-1, 84.13% - CRL-40420).

Thaken all these data togheter, we showed here a novel method of treatment for human pancreatic cancer with specifically immunolabelled gold nanoparticles with high selectivity for pancreatic cancer cells for further thermal activation by external laser field. We estimate that the proposed practical approach will allow us to advance the designed nanocompounds in phase 1 clinical trials on human patients with pancreatic cancer.

## References

- [1] Jemal A, Bray F, Center MM, Ferlay J, Ward E, Forman D. Global cancer statistics. *CA Cancer J Clin* 2011 Mar-Apr;61(2):69-90.
- [2] Patra CR, Bhattacharya R, Wang E, Katarya A, Lau JS, Dutta S, et al. Targeted delivery of gemcitabine to pancreatic adenocarcinoma using cetuximab as a targeting agent. *Cancer Res* 2008;68(6):1970-1978.
- [3] Yang F, Jin C, Subedi S, Lee CL, Wang Q, Jiang Y, et al. Emerging inorganic nanomaterials for pancreatic cancer diagnosis and treatment. *Cancer Treat Rev* 2012;38(6):566-579.
- [4] Borja-Cacho D, Jensen EH, Saluja AK, Buchsbaum DJ, Vickers SM. Molecular targeted therapies for pancreatic cancer. *Am J Surg* 2008 Sep;196(3):430-441.

- [5] Mocan L, Ilie I, Tabaran FA, Dana B, Zaharie F, Zdrehus C, et al. Surface plasmon resonance-induced photoactivation of gold nanoparticles as mitochondria-targeted therapeutic agents for pancreatic cancer. *Expert opinion on therapeutic targets* 2013(0):1-11.
- [6] Hainfeld JF, O'Connor MJ, Lin P, Qian L, Slatkin DN, Smilowitz HM. Infrared-transparent gold nanoparticles converted by tumors to infrared absorbers cure tumors in mice by photothermal therapy. *PloS one* 2014;9(2):e88414.
- [7] Iancu C, Mocan L, Bele C, Orza AI, Tabaran FA, Catoi C, et al. Enhanced laser thermal ablation for the in vitro treatment of liver cancer by specific delivery of multiwalled carbon nanotubes functionalized with human serum albumin. *International Journal of Nanomedicine* 2011;6:129.
- [8] Mocan L, Tabaran F, Mocan T, Bele C, Orza A, Lucan C, et al. Selective ex-vivo photothermal ablation of human pancreatic cancer with albumin functionalized multiwalled carbon nanotubes. *International Journal of Nanomedicine* 2011 28 April 2011;6(1):915-928.
- [9] Iancu C, Mocan L. Advances in cancer therapy through the use of carbon nanotube-mediated targeted hyperthermia. *International Journal of Nanomedicine* 2011;6:1675.
- [10] Ohno M, Oka S, Nakabeppu Y. Quantitative analysis of oxidized Guanine, 8-oxoguanine, in mitochondrial DNA by immunofluorescence method. *Methods Mol Biol* 2009;554:199-212.

